# INTEGRATING GIS AND EARTH OBSERVATION DATA IN ASSESSING LAND SUBSIDENCE CAUSED BY LARGE SEISMIC MOVEMENTS: A CASE IN SURIGAO CITY, MINDANAO, PHILIPPINES

Arnaldo C. Gagula[1,2], Kendel P. Bolanio[1,2], Monalaine M. Bermoy[1,2], Tweete Magelle G. Bisnar[1], May Ai L. Bolatete[1]
[1]Department of Geodetic Engineering, Caraga State University, Ampayon, Butuan City, 8600, Philippines
Emails: tweetemagelle.bisnar@carsu.edu.ph, mayai.bolatete@carsu.edu.ph
2Caraga Center for Geo-informatics, Caraga State University, Ampayon, Butuan City, 8600, Philippines
Emails: acgagula@carsu.edu.ph, kpbolanio@carsu.edu.ph, mmbermoy@carsu.edu.ph

**Abstract:** Large seismic movement is one of the few contributing factors to land subsidence. Such lowering of land can be measured using Differential Interferometric Synthetic Aperture Radar (DInSAR) technique on a Sentinel – 1 SAR image pairs with centimetric accuracy. This study assessed the land subsidence in Surigao City, Philippines, a seismically active area, after the most significant annual seismic movements in the years 2017, 2018, 2020, and 2021, and the two highest movements in 2019. The spatial correlation between highly subsided areas and the Philippine Fault Line has been further examined. Results of the study presented an uplift and subsidence in the area after large earthquakes with magnitudes of 3.2 to 6.7 Ms. Highest subsidence values were -7.5 to -27.4 centimeters (cm) for the five events excluding 2017, as the land surface had elevated by up to 30.7 cm; while an accumulated displacement value of up to -39.83 cm (subsidence) found in Barangay Bonifacio, 6.58 km to the fault line. Regions with LULC-crops and built areas had a significant value of subsidence. Generally, this study suggested the contribution of seismic movements to Surigao City's land subsidence as highly subsided areas co-locate the ground shaking and liquefaction-vulnerable areas.

**Keywords:** Sentinel-1, DInSAR, earthquake, fault line, LULC

## 1. INTRODUCTION

Land subsidence is the lowering of the land surface relative to a reference level, such as mean sea level (MSL) or reference ellipsoid [1], which is caused by natural and human-related activities including groundwater exploitation, loads above the ground, sea-level rise, and tectonic movements[2]. Land subsidence is an unavoidable phenomenon that causes significant destruction in a place. Mostly, this happens in urban and adjacent coastal areas, which have been recognized and measured since 1997. Notable incidents of land subsidence due to large seismic movements have been recorded across the globe, such as in Mexico City, Iran, Cyprus, and Nepal.

In history, an average of three major destructive earthquakes per year occurred in the Philippines [3]. Surigao City, one of the Philippines' seismically active areas, is very susceptible to seismic-induced damage due to the 100-km segment of the Philippine fault with a potential to generate a maximum of 7.4 magnitude earthquake [4]. On February 10, 2017, a 6.7 Magnitude (Ms) earthquake, 16 km offshore northwest of Surigao City, shook the island of Mindanao, Southern Philippines. Surigao City suffered from the most substantial ground shaking, with a PHIVOLCS Earthquake Intensity Scale (PEIS) of VII (Destructive), while neighboring municipalities were hit on a lower scale [5]. The strong-level earthquake was among the highest damage-causing earthquakes in the area, along with the 7.4 (Ms) Magnitude Surigao Earthquake in 1879.

Assessing the impact of earthquakes on both ground and features is an essential mechanism for mitigation and land use planning. Hence, with the advancement of remote sensing, satellite images such as through Sentinel-1 Terrain Observation with Progressive Scan (TOPS) can provide data containing valuable information for terrain surface deformation using interferometric measurements. Synthetic Aperture Radar (SAR) is a microwave imaging system with a cloud-penetrating capability that can capture images day and night. Using the acquired images and the process of differential interferometry, mapping of ground deformation is possible; the technique is referred to as Differential Interferometric Synthetic Aperture Radar (DInSAR). This technique has been used along with the utilization of the Global Positioning System (GPS) for ground deformation assessment and mapping.

This study has assessed the vertical displacement of Surigao City, North-eastern Mindanao, Philippines as caused by the large seismic movements in the area and its surrounding ocean from 2017 to 2021. The spatial correlation between fault line and the result ground displacement had further assessed. An integration of Geographic Information System (GIS) technique, Earth Observation data, specifically from Sentinel-1A, and DInSAR technique had been utilized in the study.

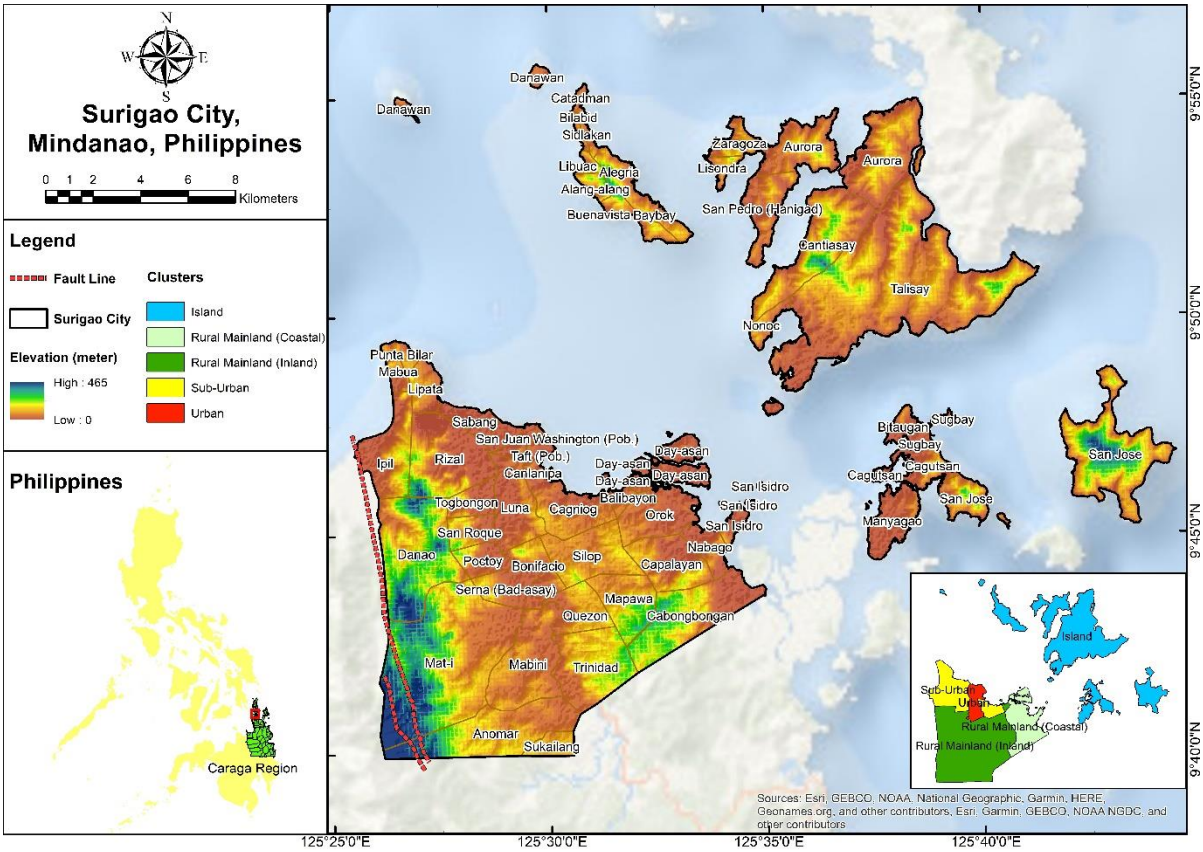


Figure 1. Location Map of Surigao City with Elevation Data (USGS) and Cluster Classification

## 2. METHODOLOGY

The assessment had employed five major activities: (i) data acquisition, (ii) SAR image data processing, (iii) land displacement analysis, (iv) land displacement maps generation, and (v) validation, refer to Figure 2.

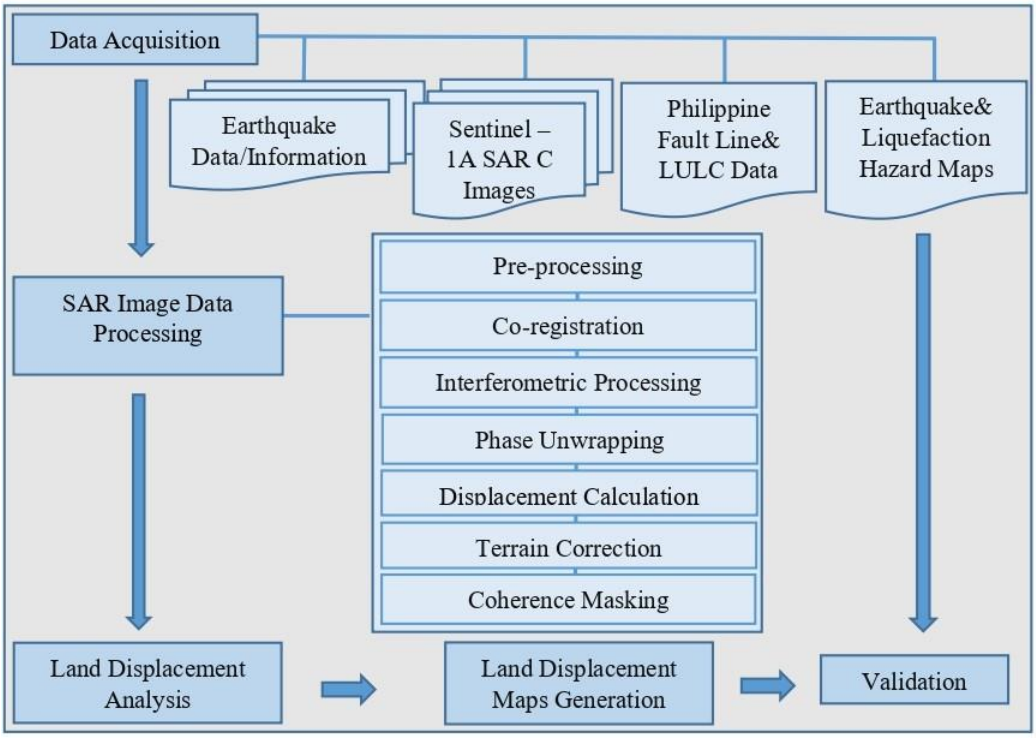


Figure 2. The Methodological Flow.

### 2.1. Data Acquisition

Earthquake data/information was gathered from the Philippine Volcanology and Seismology (PHIVOLCS); Sentinel-1A images from the European Space Agency (ESA); and fault line and liquefaction hazard maps were from the City Planning and Development of Surigao City.

### 2.2. SAR Image Data Processing

Acquired images were processed in SNAP software from ESA for DInSAR Interferometry employing seven minor processing for each SAR image pair. Pre-processing was done to obtain the fourth to sixth bursts of each image containing the study area. Co-registration was then applied to put together the master and slave images applying extreme precision better than 0.1 which subsequently calculated the coherency of the interferometric pair, implying the measure of quality of the phase information. It determines if the images have a high degree of similarity and are suitable for further interferometric processing. The interferometric processing with SRTM 1 arc-sec HGT had enable to create an interferogram in the form of interferometric fringes. The interferogram validated the existence of deformation and represented a full $2\pi$ cycle of phase change. Ground deformation in the form of phase was then converted into metric measurements through phase unwrapping in SNAPHU program and conversion tool which is Phase to displacement in SNAP software. An uplift was represented by positive values and subsidence in negative values. The terrain correction was done to compensate for the distortion in the geometric representation of the images and its projection using WGS84/UTM Zone 51N. The coherence masking was then applied to extract pixels with acceptable coherence values of at least 0.3.

### 2.3. Land Displacement Analysis

Subsequently, results were analyzed per event basis and the total of the six events (2017, 2018, June-2019, July-2019, 2020, & 2021) per cluster, barangay, and relating to Land Use/Land Cover (LULC) of the area. Moreover, spatial characteristic of high subsiding barangays was assessed regarding the location of the Philippine fault line segment near and along the area.

### 2.4. Land Displacement Maps Generation

Maps depicting the land displacements were created using the results from the interferometric processing and displacement analyses in the ArcMap 10.4 software.

### 2.5. Validation

The validation of displacement results was associated with the liquefaction and ground shaking vulnerable areas as soil liquefaction is one of the most dangerous geotechnical phenomena that can result in severe ground subsidence during an earthquake, confirmed by recent studies as subsidence and ground deformations are evident during the post-seismic stage [6]–[8], especially in loose alluvial deposits or reclaimed lands. Moreover, the coherency of the interferometric images further validated the quality of the displacement results.

## 3. RESULTS AND DISCUSSIONS

### 3.1. SAR Data Processing Results

#### 3.1.1. Coherence of Image Pairs

Coherence shows the strength of association between two SAR images and serves as a phase quality parameter measuring the phase stability of the target ground while interferogram shows the fringes of colors representing the difference in the distance to the ground between satellites or single satellite passing at different time, such difference is known as the interferometric phase.

The value of 1 corresponds to the optimum coherence of two images implying a complete absence of phase noise while decreasing value is associated with an increase in phase noise. A minimum of 0.3 coherence coefficient is acceptable for providing quality and reliable results [9]. The average coherency for each image pair was within 0.3031-0.3135, while the highest coherency of each pixel was between 0.993-0.973 and the lowest at 0.077-0.096. Pixels with highest recorded coherency (0.987-0.993) were from image pairs taken during optimal weather conditions. High coherent areas were in land use/land cover classes – built area, bare ground, and rangeland, where scatterers are more stable. Moreover, errors in the interferometry were estimated within the range 0.00098-0.00099.

The following figures show the coherency of the master and slave images for each used image pair.

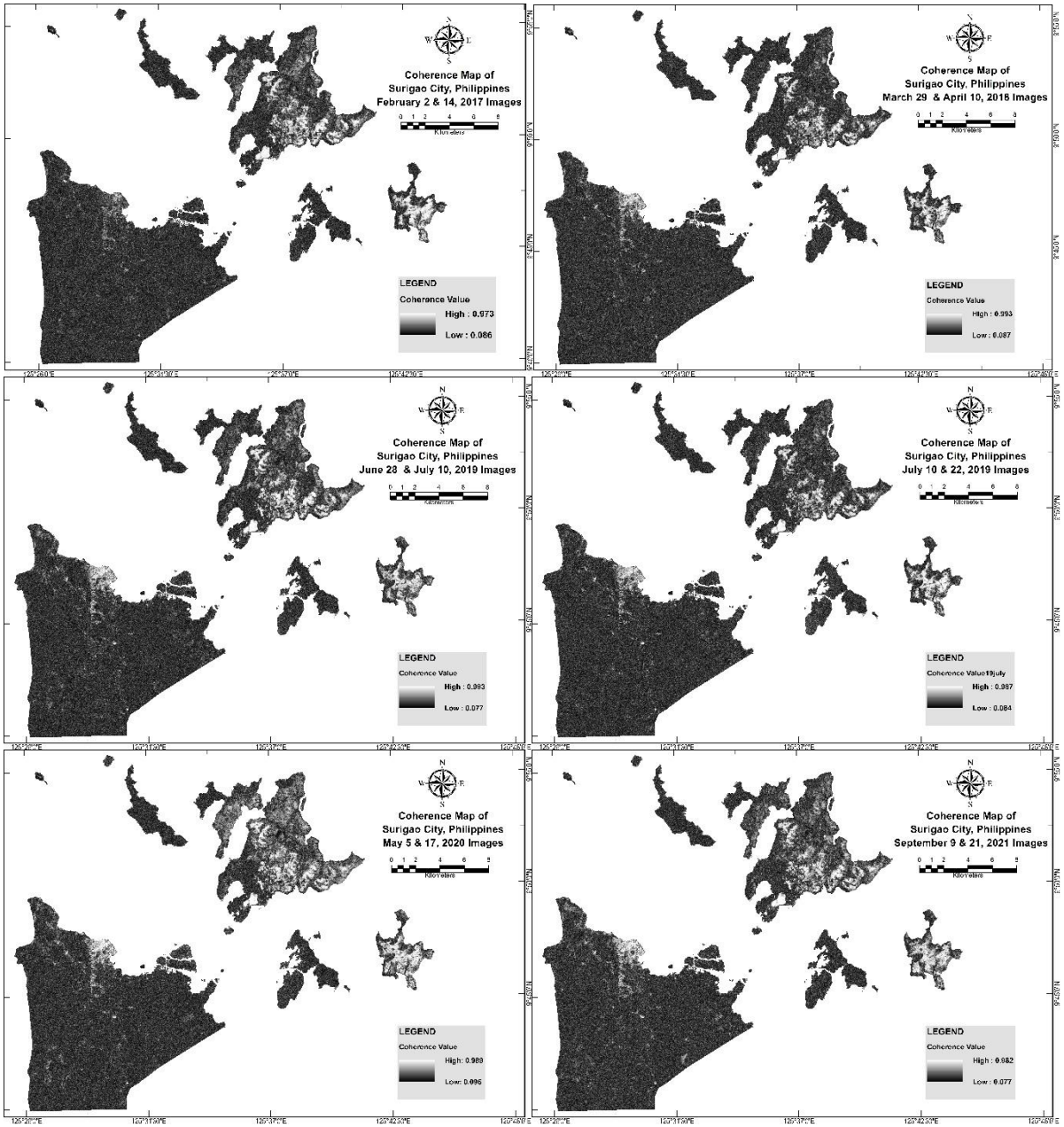


Figure 3. Coherency Maps of the Interferometric Image Pair for 2017, 2018, June-2019, July-2019, 2020, and 2021

### 3.1.2. Interferograms

The following set of figures is the interferograms generated for each considered event. Patterns of fringes were seen, particularly in areas with high coherency. Closer fringes indicate larger deformation value, while constant or slowly varying fringes implies a flat terrain. Sentinel-1A C-band operates at 5.405 GHz with a corresponding wavelength of approximately 5.55 cm.

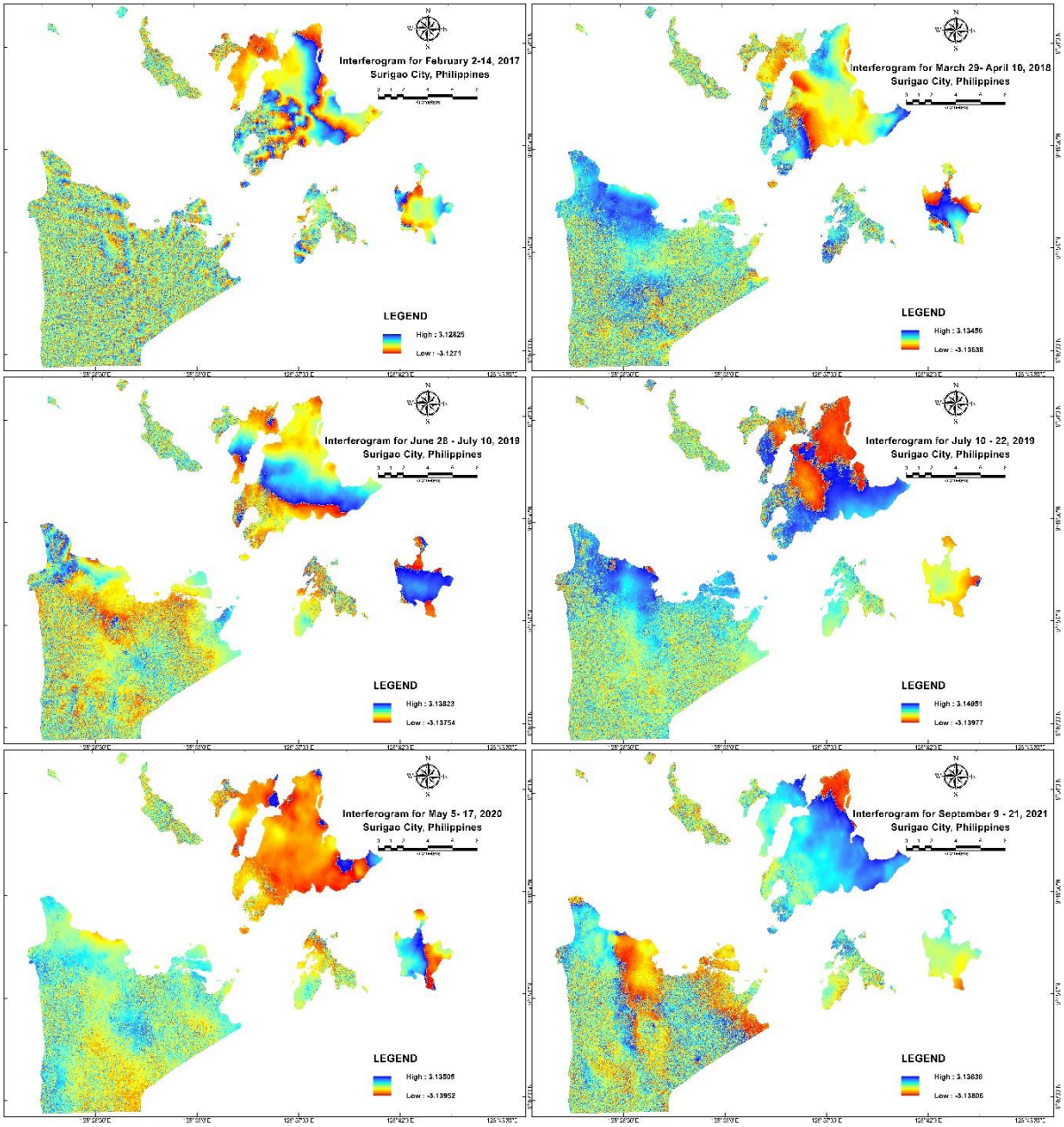


Figure 4. Interferograms for the Six Events

### 3.2. Land Displacement Results

#### 3.2.1. Displacement of Surigao City for the Six Events

Generally, the highest subsidence values were 7.5-27.4 cm for the five (5) events excluding in 2017 as land surface had elevated by up to 30.7 cm. Results show the vertical displacement, both uplift and subsidence, in the area of Surigao City after an earthquake events. Similar recent studies, measuring land subsidence due to seismic movements, came up with values -3.1 cm and 7.4 cm [10], -33 cm to -61 cm [11], -41 cm and 90 cm. While, previous land subsidence measurements in the area within the period of one year from April 27, 2017 to April 10, 2018, an uplift of up to 9.8 cm and subsidence of up to -14.6 cm were measured which being associated to groundwater extraction. However, the result of this assessment, particularly the second event dated March 29 to April 10, 2018, land subsidence was in magnitude of up to -27.4 cm.

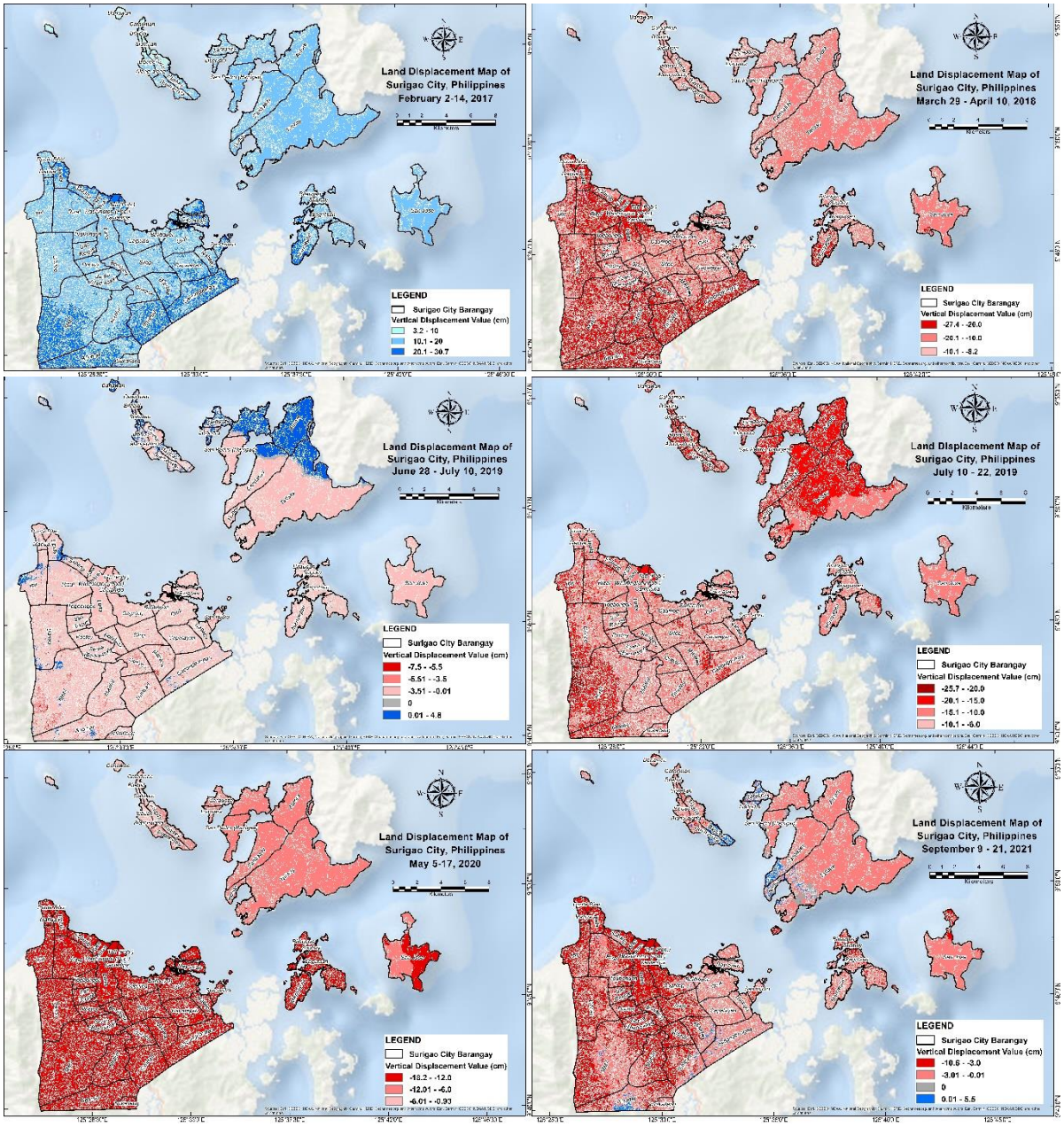


Figure 5. Land Deformation Maps of Surigao City (2017- 2021)

The following graphs show the relationships between displacement and the four (4) influencing factors – magnitude of earthquake, number of earthquakes, depth of earthquake's focus, and distance of earthquake's epicenter from Surigao City mainland.

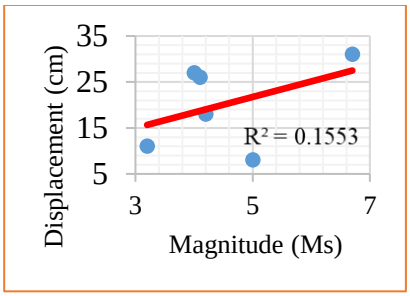


(a)Direct Relation between Displacement and Earthquake Magnitude

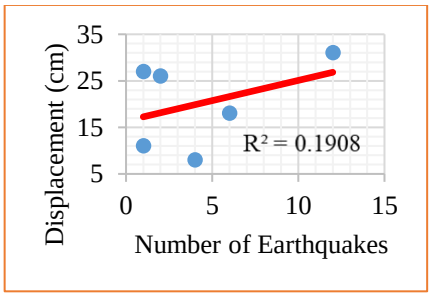


(b) Direct Relation between Displacement and Number of Earthquake

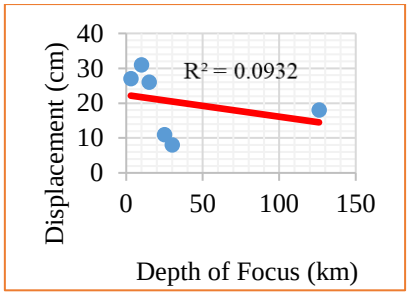


(c)Indirect Relation between Displacement and Depth of Focus

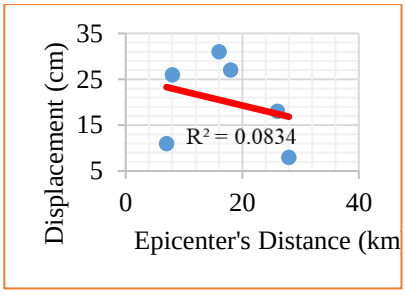


(d) Indirect Relation between Displacement and Earthquake Epicenter's Distance

### 3.2.2. Total Displacement of Surigao City Clusters

The Urban cluster was the most subsiding with total subsidence of 38.35 cm, followed by Sub-Urban with 36.49 cm, Rural Mainland (Inland) with 36.48 cm, Rural Mainland (Coastal) with 32.36 cm, and the Island cluster having the lowest total subsidence with 29.30 cm for the six events. Land displacements were affected by different factors present in the area, such as different loads above the ground during the pre and post-events and the continuing water extraction from the deep wells and other water resources [12].

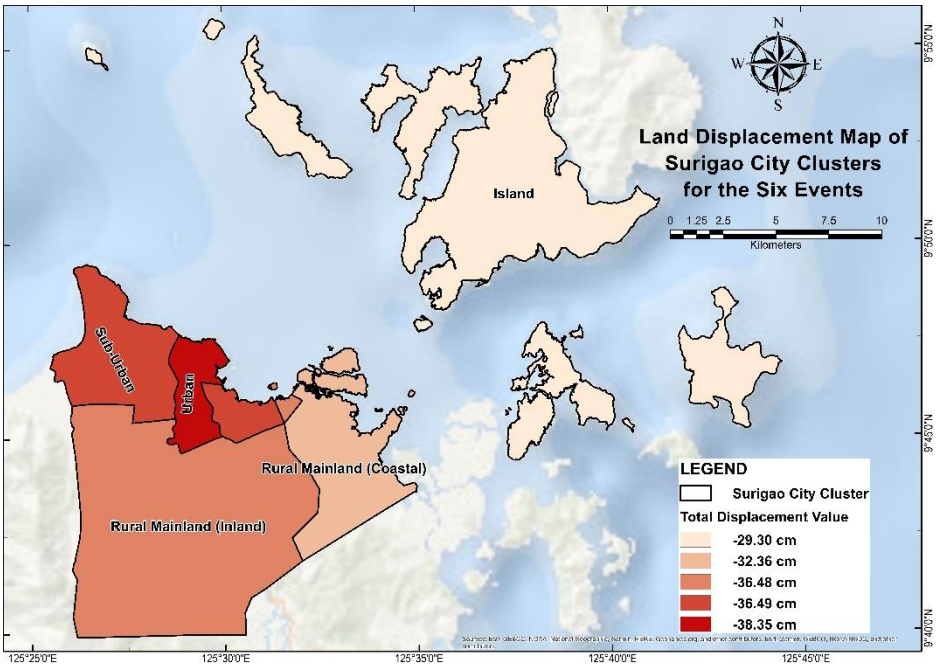


Figure 6. Land Displacement Map of Surigao City Clusters for the Six Events

### 3.2.3. Total Displacement of Surigao City Barangays

The ten (10) highest subsiding barangays include Bonifacio, Luna, Togbongon, San Roque, Quezon, and Danao; including Mabini, Canlanipa, Poctoy, and Serna, where water extraction had done in the reservoirs and deep wells in the area. Moreover, barangays Rizal, Cagniog, Taft, and Lipata, with high subsidence values, have existing dams and reservoirs as some of the city's water sources. Subsidence in these areas was also affected by the water extraction activities.

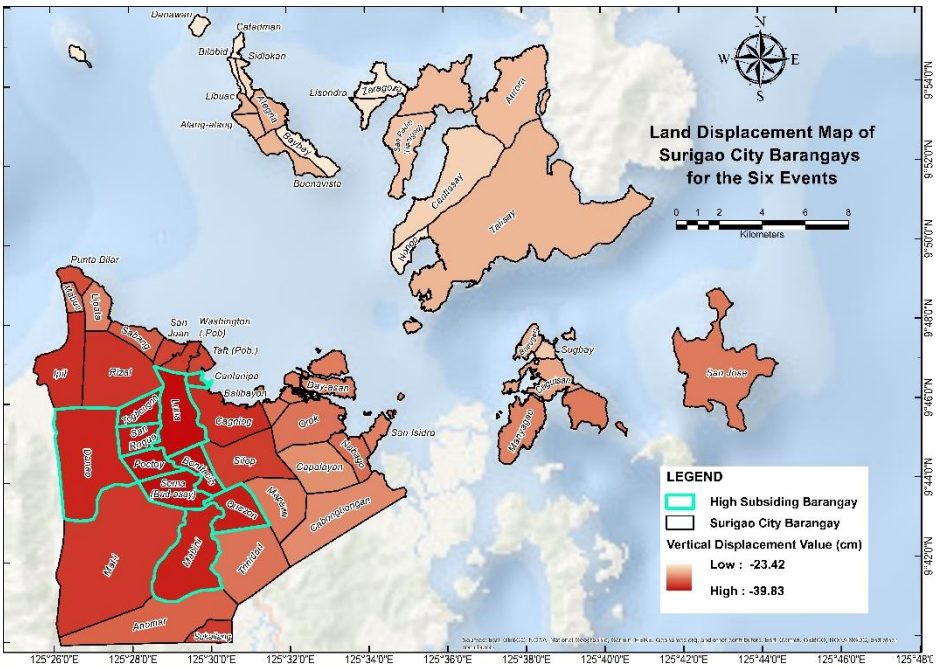


Figure 7. Land Displacement Map of Surigao City Barangays for the Six Events

### 3.2.4. Total Displacement of Surigao City per Land Cover/Land Use Class

Classes of LULC (arranged in descending order based on subsidence value), crops, built area, trees, bare ground, water, flood vegetation, and rangeland had subsided by 37.04 cm, 36.17 cm, 33.21 cm, 32.04 cm, 31.80 cm, 30.86 cm, and 30.28 cm, respectively.

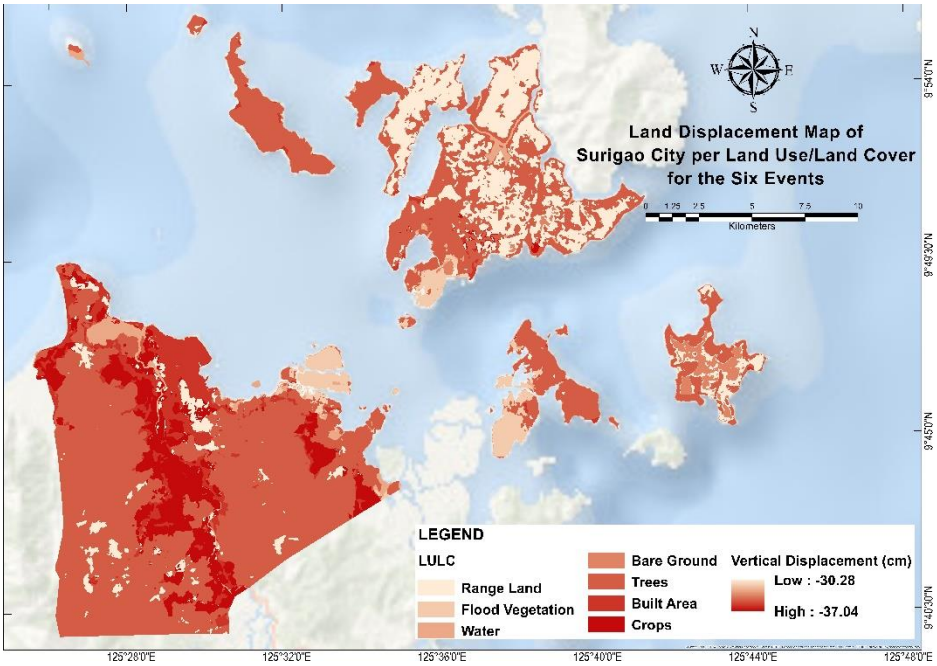


Figure 8. Land Displacement Map of Surigao City per LULC for the Six Events

### 3.2.5. Surigao City's High Subsiding Barangays and Its Spatial Correlation to the Philippine Fault Line Segment

Results further suggested that barangays along and near the fault line had higher subsidence values than farther barangays.

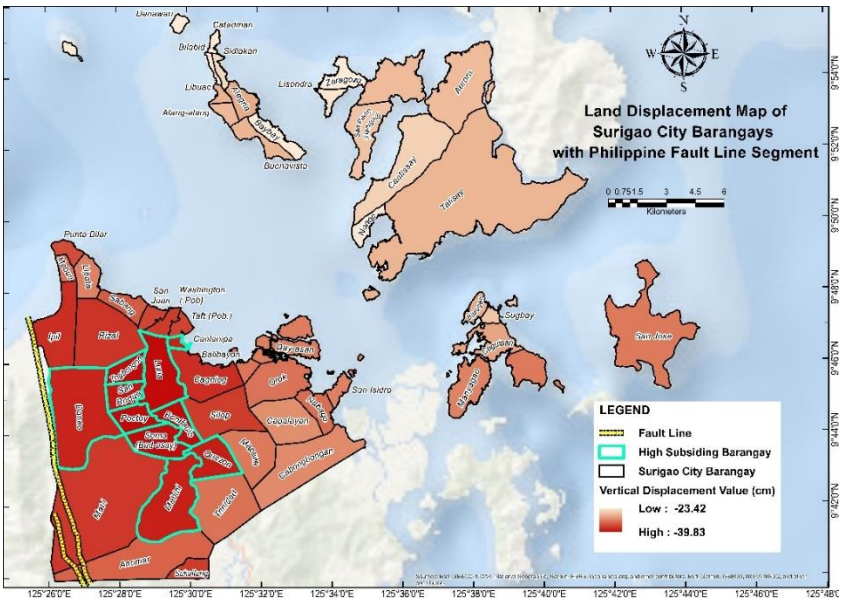


Figure 9. Land Displacement Map of Surigao City Barangays for the Six Events with the Philippine Fault Line Segment

### 3.6 Validation Results

High subsiding areas/barangays are within the vulnerable classified areas for liquefaction. The top 10 highest subsiding barangays are in the mainland susceptible to PEIS VII & above earthquake intensities, with 35% of the area vulnerable to liquefaction (refer to figure10). Specifically, high subsiding areas at the center of Surigao City Mainland during the September 9-21, 2021 measurement, as shown in figure 10, match the liquefaction–prone areas. Thus, this correlation validated the land subsidence phenomenon in the area due to seismic movements as soil liquefaction resulting from ground shaking can induce land subsidence. Moreover, the quality of DInSAR results was assured as standard coherency of stacked images has been met, utilizing pixels with coherence values of 0.3 and above.

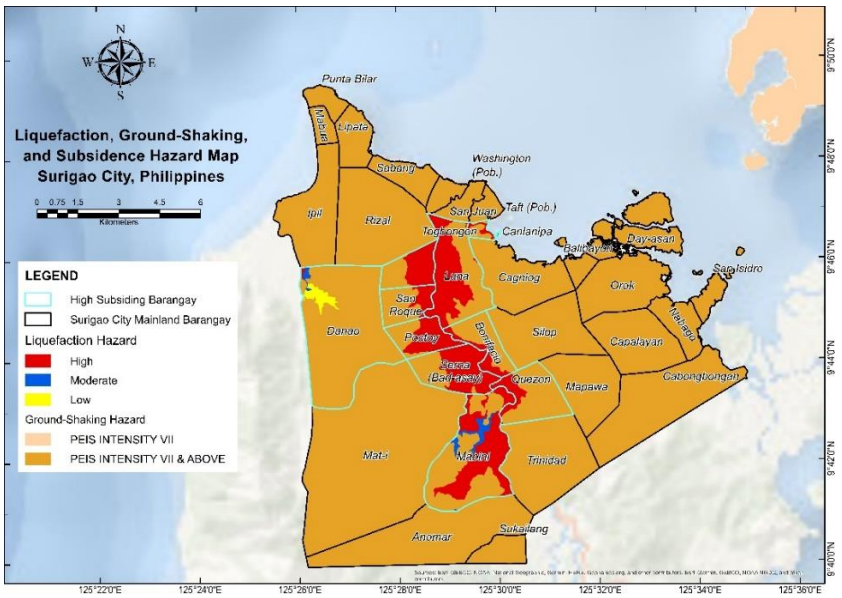


Figure 10. Map of Liquefaction, Ground-Shaking, and High Subsiding Vulnerable Areas of Surigao City, Philippines

## 4. CONCLUSIONS AND RECOMMENDATIONS

### 4.1. Conclusions

The study proved that seismic movements could contribute to the land's vertical displacement, whether uplift or subsidence, particularly barangays near the fault line and earthquake epicenters. The highest measured subsidence values were 7.5 cm to 27.4 cm for the five (5) events excluding in 2017 as the entire land surface had elevated by up to 30.7 cm. Barangays Bonifacio, Poctoy, Luna, Serna, Togbongon, San Roque, Quezon, Mabini, Canlanipa, and Danao were the ten highest subsiding barangays with accumulated subsidence values of 37.83 cm to 39.83 cm, located in the mainland of Surigao City and near the Philippine Fault Line segment, additionally covering the liquefaction vulnerable area.

The association of land use/land cover further proved the presence of land subsidence as built area with high coherency, implying less presence of limiting factors of measurement, was the second highest subsiding area. Moreover, earthquake's magnitude, number of earthquakes, depth of focus, and epicenter distance from the area are factors of earthquake-induced land displacement, as displacement magnitudes varied in the six events.

### 4.2. Recommendations

The study focuses on measuring vertical displacement of Surigao City during the large seismic events using pair of images acquired in the pre- and post-event with a temporal resolution of 12 days and a DInSAR technique. Given the findings and conclusions of the assessment, the researchers recommend to Utilization of advanced methodologies like Satellite-Based Augmentation (SBAS) and Persistent Scatterer Interferometric Synthetic Aperture Radar (PSInSAR) to generate a more precise map of vertical displacement and assess other influencing factors of land subsidence in the area and the spatial distribution and thickness of sediments using gravimetric data and correlating to the prevalent land subsidence.

## 5. REFERENCES


[1] H. Z. Abidin, H. Andreas, I. Gumilar, T. P. Sidiq, and Y. Fukuda, "On the roles of geospatial information for risk assessment of land subsidence in urban areas of Indonesia," in *Lecture Notes in Geoinformation and Cartography*, 2013, vol. 0, no. 199609, doi: 10.1007/978-3-642-33218-0_19.

[2] Y. Shi, D. Shi, and X. Cao, "Impacting factors and temporal and spatial differentiation of land subsidence in Shanghai," *Sustain.*, vol. 10, no. 9, 2018, doi: 10.3390/su10093146.

[3] S. R. Calumba, M. Rith, and A. M. Fillone, "Earthquake evacuation choice and management in a developing archipelagic country—a case study of Surigao city, Philippines," *Sustain.*, vol. 13, no. 11, 2021, doi: 10.3390/su13115783.

[4] J. S. Perez, H. Tsutsumi, M. T. Cahulogan, D. P. Cabanlit, M. I. T. Abigania, and T. Nakata, "Fault distribution, segmentation and earthquake generation potential of the philippine fault in eastern mindanao, philippines," *J. Disaster Res.*, vol. 10, no. 1, pp. 74–82, 2015, doi: 10.20965/jdr.2015.p0074.

[5] "PRIMER ON THE 10 FEBRUARY 2017 MAGNITUDE 6.7 EARTHQUAKE AT SURIGAO DEL NORTE." https://www.phivolcs.dost.gov.ph/index.php/news/619-primer-on-the-10-february-2017-magnitude-6-7-earthquake-at-surigao-del-norte (accessed Dec. 10, 2021).

[6] K. Kajihara, R. M. Pokhrel, T. Kiyota, and K. Konagai, "Liquefaction-induced ground subsidence extracted from Digital Surface Models and its application to hazard map of Urayasu city, Japan," *15th Asian Reg. Conf. Soil Mech. Geotech. Eng. ARC 2015 New Innov. Sustain.*, no. July 2019, pp. 829–834, 2015, doi: 10.3208/jgssp.TC203-02.

[7] R. Rasouli and A. F. Wheeler, "EXPERIMENTAL STUDY ON SUBSIDENCE OF SURFACE STRUCTURES DUE TO LIQUEFACTION," no. October, 2014.

[8] Y. Huang and X. Jiang, "Field-observed phenomena of seismic liquefaction and subsidence during the 2008 Wenchuan earthquake in China," *Nat. Hazards*, vol. 54, no. 3, pp. 839–850, 2010, doi: 10.1007/s11069-010-9509-6.

[9] A. Braun and L. Veci, "Sentinel-1 Toolbox Interferometry Tutorial," no. May 2014, pp. 1–20, 2015, [Online]. Available: http://www.ggki.hu/~banyai/S1TBX/S1TBX Stripmap Interferometry with Sentinel-1 Tutorial.pdf.

[10] M. Tzouvaras, D. Kouhartsiouk, A. Agapiou, C. Danezis, and D. G. Hadjimitsis, "The use of Sentinel-1 synthetic aperture radar (SAR) images and open-source software for cultural heritage: An example from paphos area in Cyprus for mapping landscape changes after a 5.6 magnitude earthquake," *Remote Sens.*, vol. 11, no. 15, pp. 1–13, 2019, doi: 10.3390/rs11151766.

[11] T. Priya and A. C. Pandey, "Geoinformatics-based assessment of land deformation and damage zonation for Gorkha earthquake, 2015, using SAR interferometry and ANN approach," *SN Appl. Sci.*, vol. 3, no. 5, 2021, doi: 10.1007/s42452-021-04574-9.

[12] City Planning and Development Office, "Surigao City Ecological Profile," 2017, [Online]. Available: http://www.surigaocity.gov.ph/sites/default/files/documents/content/surigao_city_ecological_profile_2016.pdf.